Electronic Supplementary Material (ESI) for Analyst.

Halogen-Modified Carbazole Derivatives for Lipid Droplet-Specific Bioimaging and Two-Photon Photodynamic Therapy

Wenli Du,[a,†] Xin Lu,[a,†] Tong Yuan,[c,†] Zhimin Sun,[b] Xiaocheng Li,[a] Shengli Li,[a] Qiong Zhang,[a] Xiaohe Tian,[e] Dandan Li,[b]* and Yupeng Tian [a,d]*

[a] *Department of Chemistry, Key Laboratory of Functional Inorganic Material Chemistry of Anhui Province, Anhui University, Hefei 230039, P. R. China*

[b] *Institutes of Physics Science and Information Technology, Key Laboratory of Structure and Functional Regulation of Hybrid Materials, Ministry of Education, Anhui University, Hefei 230601, P. R. China*

[c] *School of Life Science, Anhui University, Hefei 230601, P. R. China*

[d] *State Key Laboratory of Coordination Chemistry, Nanjing University*

[e] *Huaxi MR Research Centre (HMRRC), Department of Radiology; Functional and Molecular Imaging Key Laboratory of Sichuan Province, West China Hospital of Sichuan University, Chengdu, China, 610041, China.*

† These authors contributed equally to this work

*Corresponding author: chemlidd@163.com; yptian@ahdu.eu.cn

1.1 Materials and Apparatus

The general chemicals were obtained from Aladdin industrial corporation (China) and Macklin (China) and used without further purification. Calcein-AM/PI Double Stain Kit, Annexin V-FITC/PI Apoptosis Detection Kit and HCS LipidTOX™ Deep Red Sain were obtained from Shanghai Bestbio (China). The solvents were dried and distilled according to standard procedures. ^{1}H-NMR spectra were performed on a Bruker 400 Hz Ultra shield spectrometer and reported as parts per million (ppm) from TMS (δ), ^{13}C-NMR spectra were obtained on a Bruker Advance 100 MHz NMR spectrometer. UV-*vis* absorption spectra were recorded on a UV-265 spectrophotometer. Fluorescence measurements were carried out on a Hitachi F-7000 fluorescence spectrophotometer.

1.2 Computational details.

The ground states for each molecule were calculated using the density functional theory level with the B3LYP functional employing a 6-31G* and lanl2dz basis set. The absorption energies were investigated by time-dependent density functional theory (TD-DFT). All calculations were performed by the use of the Gaussian 09 suite of programs.[1]

1.3 Two-photon absorption cross-section.

Two-photon absorption cross-sections of **C-H**, **C-Br** and **C-I** were obtained by the two-photon excited fluorescence (TPEF) method at femtosecond laser piles and a Ti: sapphire system (680-1080 nm, 80 MHz, 140 fs) as the light source. Two-photon absorption cross-section (δ) values were determined by the following equation:

$$\delta = \delta_{ref} \frac{\Phi_{ref}}{\Phi} \frac{c_{ref}}{c} \frac{n_{ref}}{n} \frac{F}{F_{ref}}$$

The subscripts ref stands for the Fluorescein. Φ is the quantum yield, n is the refractive index, F is the integrated area under the corrected emission spectrum, c is the concentration of the solution in mol·L^{-1}. The δ_{ref} value of reference was taken from the literature.[2]

1.4 Cell imaging.

HeLa cells were seeded in 24-well glass bottom plate at a density of 2×10^4 cells per well and grown for 96 h. For live cell imaging, cell cultures were incubated with the complexes (10% PBS: 90% cell media) at concentration 4 μM and maintained at 310 K in an atmosphere of 5% CO_2 and 95% air for incubation times ranging for 30 min. The cells were then washed with PBS (3 × 1 mL per well) and 1 mL of PBS was added to each well. The cells were imaged using confocal laser scanning microscopy using oil immersion lenses.

1.5 STED imaging.

STED nanoscopy experiments were performed under a Leica DMi8 confocal microscope equipped with a Leica TCS SP8 STED-ONE unit, the compound was excited under an STED laser, and the emission signals were collected using HyD reflected light detectors. Specimen living cells were prepared using a method similar to normal confocal microscopy described previously. The STED micrographs were further processed using deconvolution wizard function using Huygens Professional software (version: 16.05) under authorized license.

1.6 Cytotoxicity test.

The effects of **C-H**, **C-Br** and **C-I** on viability of cells were carried out using the methylthiazolyldiphenyl-tetrazolium bromide (MTT) assay. Hela cells were trypsinized and plated to 70% confluence in 96 well plates 24 h before treatment. Prior to the compounds' treatment, the DMEM was removed and replaced with fresh DMEM, and aliquots of the **C-H**, **C-Br** and **C-I** stock solutions were diluted to obtain the final concentrations of 1, 5, 10, 15, 20 μM. The treated cells were then incubated at 310 K in 5% CO_2 for 24 h. Subsequently, the cells were treated with 5 mg/mL MTT (10 μL per well) and incubated for an additional 4 h (310 K, 5% CO_2). Then, DMEM was removed, the formazan crystals were dissolved in DMSO (100 μL per well), and the absorbance at 490 nm using a microplate reader (SpectraMax Paradigm). The absorbance measured for an untreated cell population under the same experimental conditions was used as the reference point to establish 100% cell viability. Duplicated experiments have been tested.[3]

1.7 Calculation of Log P value.

1 mg of **C-H, C-Br** and **C-I** is dissolved in 5 mL n-caprylic alcohol, the supernatant (3mL) is took and blended with water (3 mL). The resulting solution is shocked for 30 min. The absorbance of alcohol layer and water layer is measured, respectively. The value of Log P = Log (absorbance of alcohol layer/absorbance of water layer).

1.8 Singlet oxygen ($^1O_2$) detection.

In this study, the amount of singlet oxygen was detected by a singlet oxygen sensor named 9,10-anthracenedipropanoic acid (ABDA), because the newly generated singlet oxygen could cause an absorbance decrease of the chemical probe at around 378 nm.[4] ABDA (100 μM) and **C-H, C-Br** and **C-I** (10 μM) were incubated together and exposed to white light irradiation for 0-5 min (the laser beam was purchased from Xian Midriver Optoelectronics Technology Co., Ltd, China.). The absorbance of the probe was measured at the same time-scale to evaluate the generation of singlet oxygen in different samples.

1.9 ROS generation detection.

DCFH-DA was used as the ROS-monitoring agent. In the experiments, 10 μL of DCFH-DA stock solution (1.0 mM) was added to 2 mL of **C-H, C-Br** and **C-I** (10 μM) and 100 μL of PBS was added, and light (100 mW/cm^2) was employed as the irradiation source. The emission of DCFH-DA at 525 nm was recorded at various irradiation times.[4,5]

1.10 Singlet Oxygen Quantum Yield (Φ_{ps}).

The relative Φ_{ps} values of **C-H, C-Br** and **C-I** were measured by the standard method using ABDA as the $^1O_2$ indicator and Rose Bengal (RB) (Φ_{ps} = 0.75) as the standard in water. In these experiments, 15 mL of ABDA solution (15 mM) was added to 3 mL of micelles solution, and the light with a power density of 100 mW /cm^2 was used as the irradiation source. The absorbance of ABDA at 380 nm was

recorded at different irradiation times to obtain the decay rate of the photosensitizing process. The $^1O_2$ quantum yield of the PS in water (Φ_{PS}) was calculated using the following formula:

$$\Phi_{PS} = \Phi_{RB}\frac{K_{PS}A_{RB}}{K_{RB}A_{PS}},$$

Here, where K_{PS} and K_{RB} are the decomposition rate constants of ABDA by the PSs and RB, respectively. A_{PS} and A_{RB} represent the light absorbed by the PSs and RB, respectively, which are determined by integration of the areas under the absorption bands in the wavelength range of 400-700 nm.[4]

1.11 Electron spin resonance (ESR) assay.

The ESR measurements were carried out with a Bruker Nano X-band spectrometer at 298K. The spin adducts of the complexes were detected using three settings as follows: 1 G field modulation, 20 mW microwave power, and 100 G scan range. The spin traps 2,2,6,6-tetramethylpiperidine (TEMP for trapping $^1O_2$, 20 mM) was used to verify the formation of reactive oxygen species (ROS) generated by **C-I** (10 μM). The ESR signals of the **C-I** (10 μM) before and after the light irradiation (100 mW/cm^2) were recorded.[6]

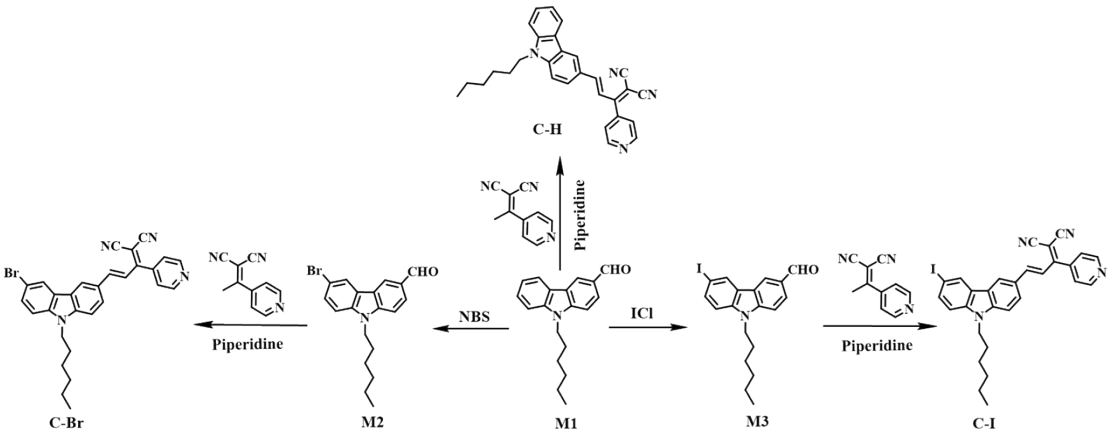

Scheme S1. Synthesis scheme for compounds **C-H**, **C-Br** and **C-I**.

1.12 Synthesis of M1:

$POCl_3$ 30.7 g (0.20 mol) was added dropwise in DMF (5.84 g, 0.08 mol) in ice-salt baths, then 10 g (0.04 mol) hexyl carbazole was dissolved in chloroform completely and then added successively. The reaction was stirred at 70 ℃ for 6 h. The mixture was cooled to room temperatur. Adjusting pH to neutral and extracting by CH_2Cl_2, and then concentrated removing solvent to crude product. Purified by column chromatography (petroleum ether: ethyl acetate = 10:1), obtaining product 7.98 g. yield 71.4 %. HRMS (ESI-MS) m/z: calcd for $C_{29}H_{26}N_4$ = 279.16, found 280.17 [M+H^+].

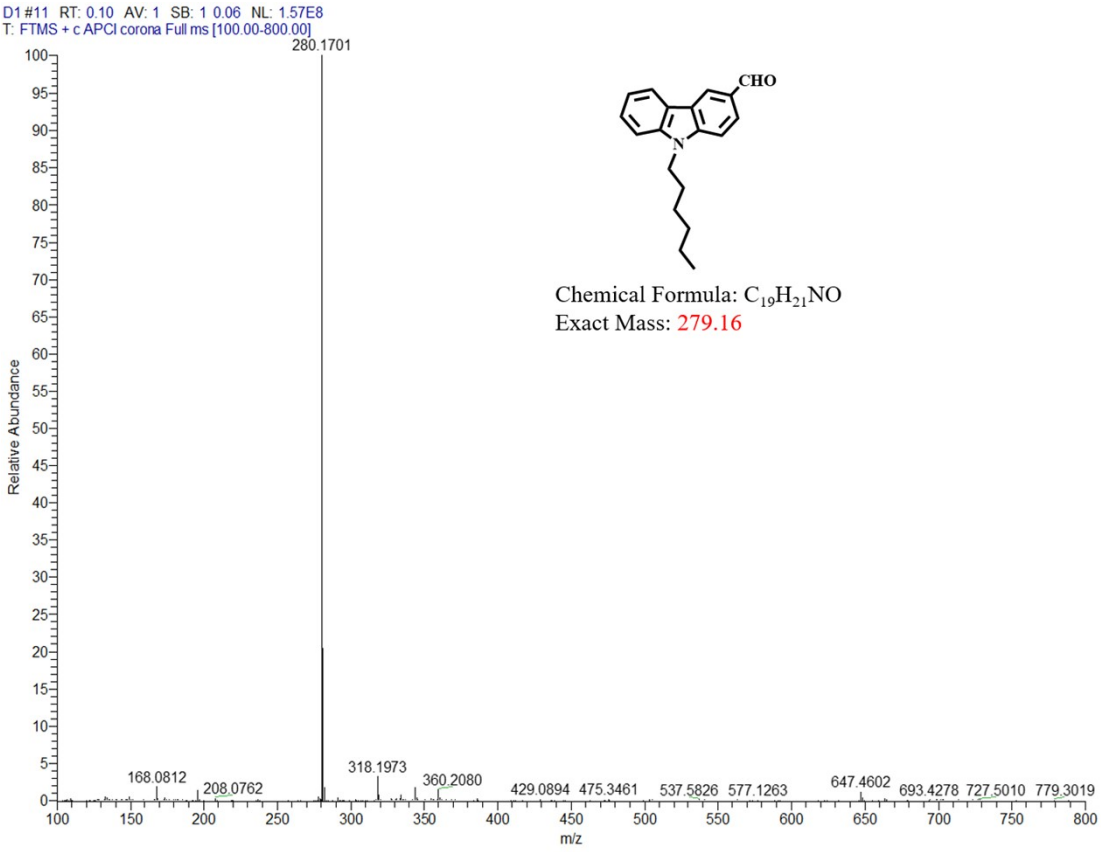

Fig S1. HRMS spectrum of **M1.**

1.13 Synthesis of M2:

Add **M1** (10.0 g, 0.04 mol), N-bromosuccinimide (NBS, 7.9 g, 0.045 mol), chloroform (100 mL) and glacial acetic acid (100 mL) in turn in a 500 mL round bottom flask, Stir at room temperature for 12 h. The reaction solution was added to 300 mL of saturated brine, the pH was adjusted to neutral with an aqueous Na_2CO_3 solution, extracted with dichloromethane, the organic phase was dried with Na_2SO_4, and the solvent was spin-dried. The crude product was purified by column chromatography (eluent: pure petroleum ether) to obtain 5.5 g of white solid, yield: 36%. ESI-MS: m/z: calcd for $C_{19}H_{20}BrNO$: 357.07, found: 358.07 [$M+H^+$].

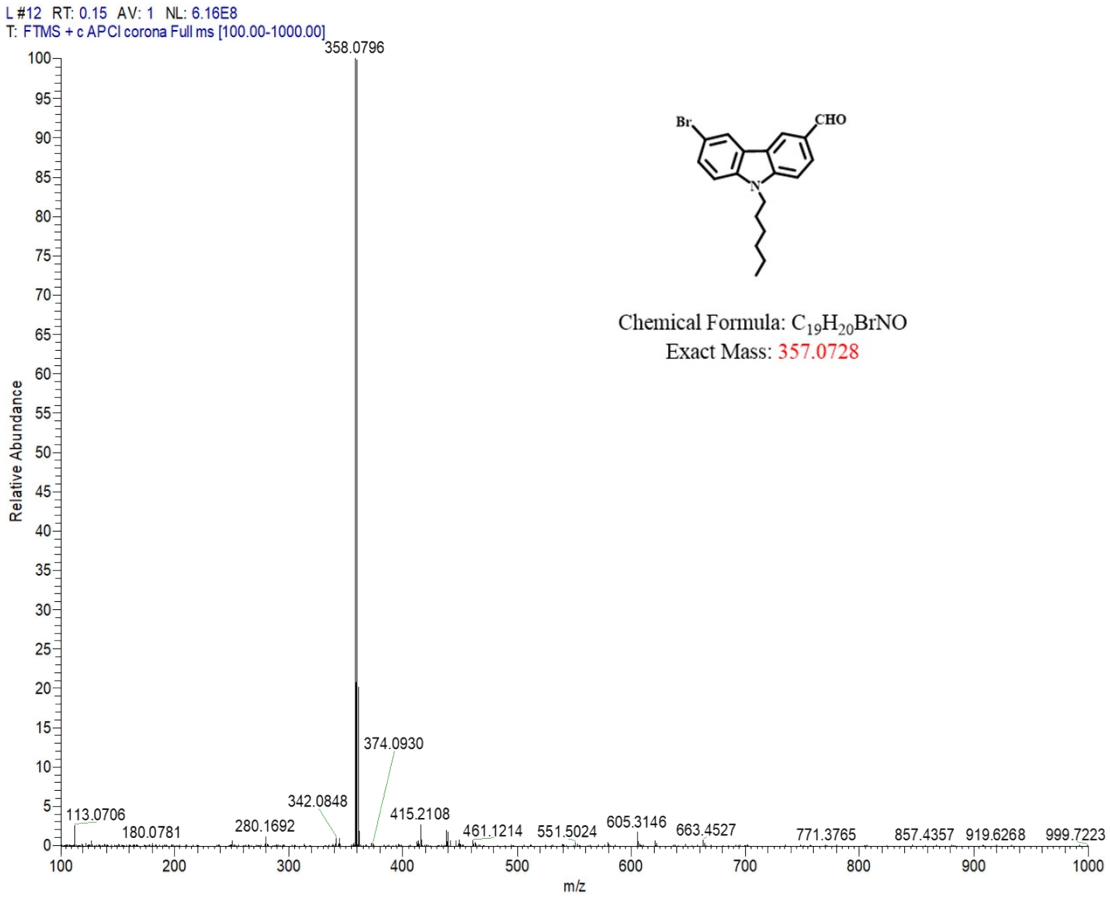

Fig S2. HRMS spectrum of **M2.**

1.14 Synthesis of M3:

Add 10.0 g (0.04 mol) of **M1** and absolute ethanol (20 mL) to a 250 mL three-necked flask, and heat and stir to dissolve it. Weigh 6.4 g (0.04 mol) of ICl and dilute it with 50 mL of absolute ethanol. Place it in a constant pressure funnel and slowly drop it into **M1**. After the addition is complete, reflux for 8 h. Distill off the ethanol to obtain a dark oil. Disperse with KI aqueous solution. The product was obtained by suction filtration 10.6 g, yield: 75%. SI-MS: m/z: calcd for $C_{19}H_{20}INO$: 405.06, found: 406.06 [$M+H^+$].

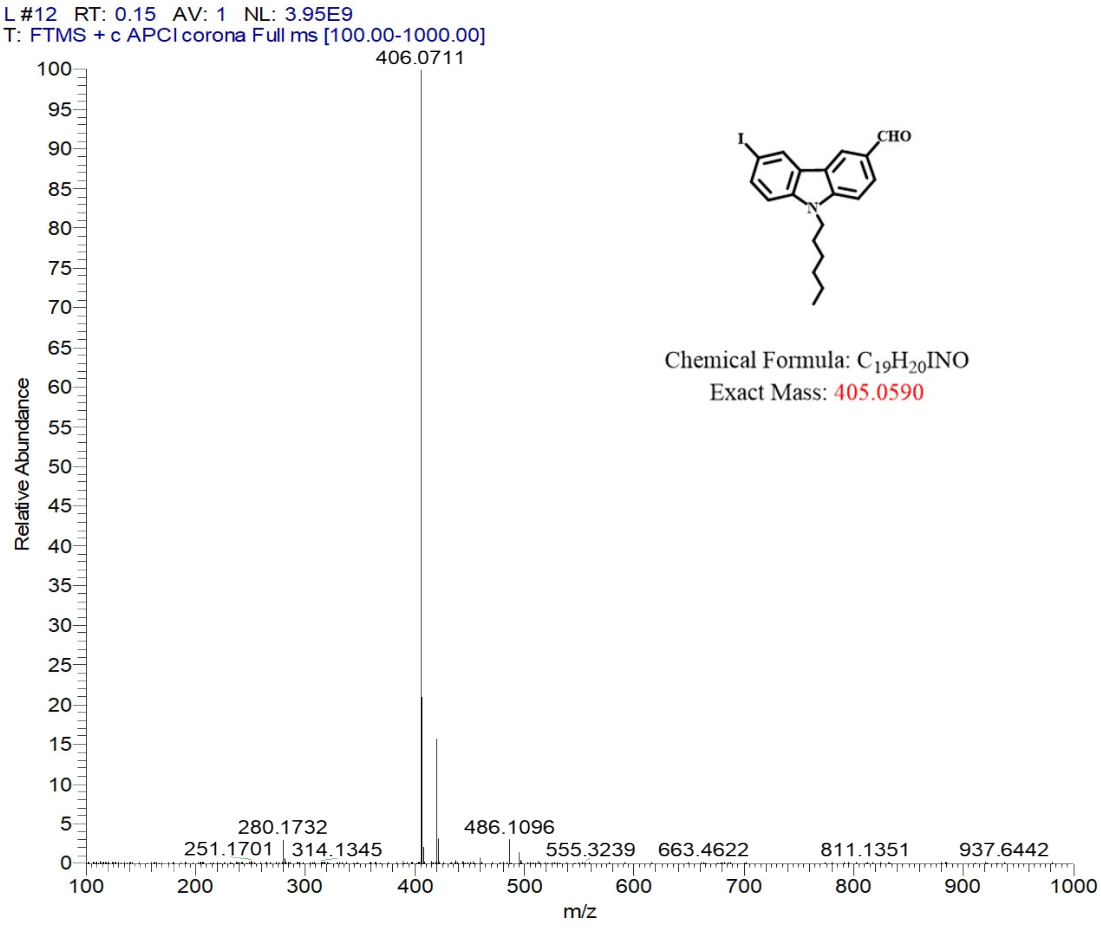

Fig S3. HRMS spectrum of **M3**.

1.15 Synthesis of C-H:

A mixture of **M1** (2.0 g, 7.10 mmol) and dicyanopyridine (1.45 g, 8.60 mmol)

were refluxed in ethanol catalyzed by a small amount of piperidine for 12 h. Purified by column chromatography (petroleum ether : ethyl acetate = 50 : 1), 1.8 g of orange-red solid was obtained. Yield: 53%. M.p.156-158 °C. ^{1}H NMR (400 MHz, DMSO-d_6) (**Fig S3**) δ 8.82 (d, J = 6.0 Hz, 2H), 8.54 (d, J = 1.7 Hz, 1H), 8.18 (dd, J = 7.7, 0.9 Hz, 1H), 7.85 (dd, J = 8.8, 1.8 Hz, 1H), 7.67-7.59 (m, 2H), 7.59-7.51 (m, 3H), 7.46 (dd, J = 8.3, 7.2, 1.2 Hz, 1H), 7.25-7.20 (m, 1H), 7.06 (d, J = 15.4 Hz, 1H), 4.38 (t, J = 7.1 Hz, 2H), 1.72 (t, J = 7.2 Hz, 2H), 1.24-1.15 (m, 6H), 0.75 (t, J = 7.1 Hz, 3H). HRMS (ESI-MS) m/z: calcd for $C_{29}H_{26}N_4$ = 430.21, found 430.21 (**Fig S4**).

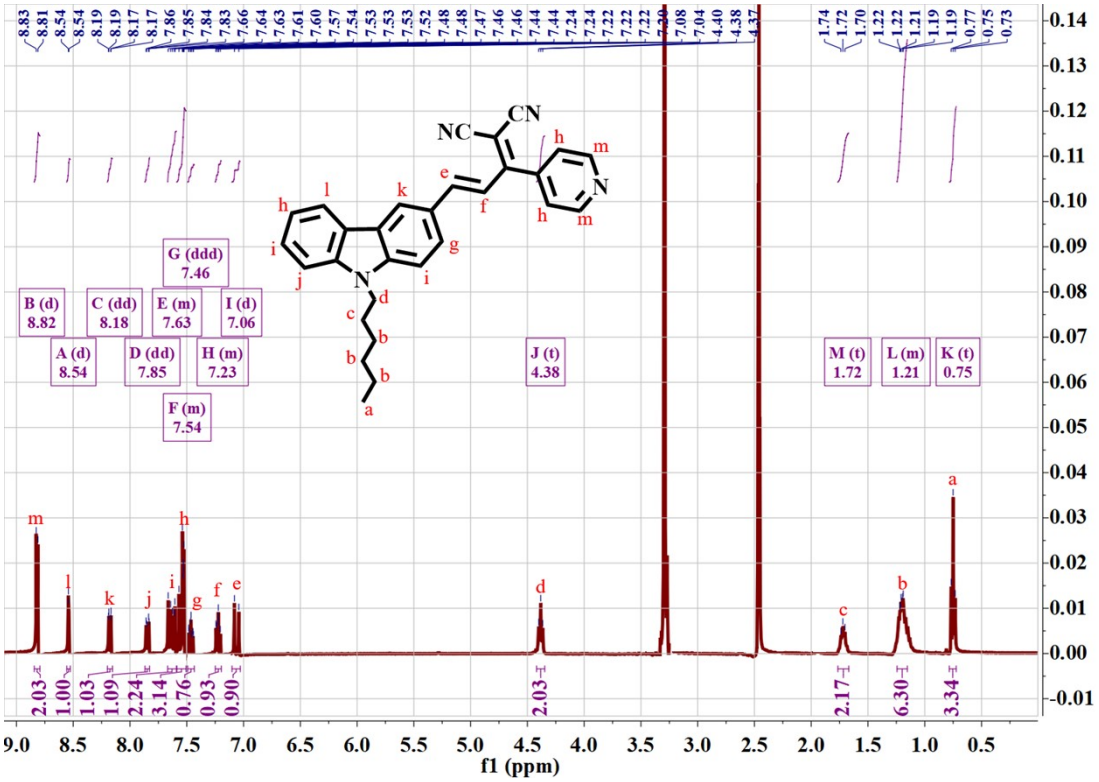

Fig S4. ^{1}H NMR spectrum of **C-H**.

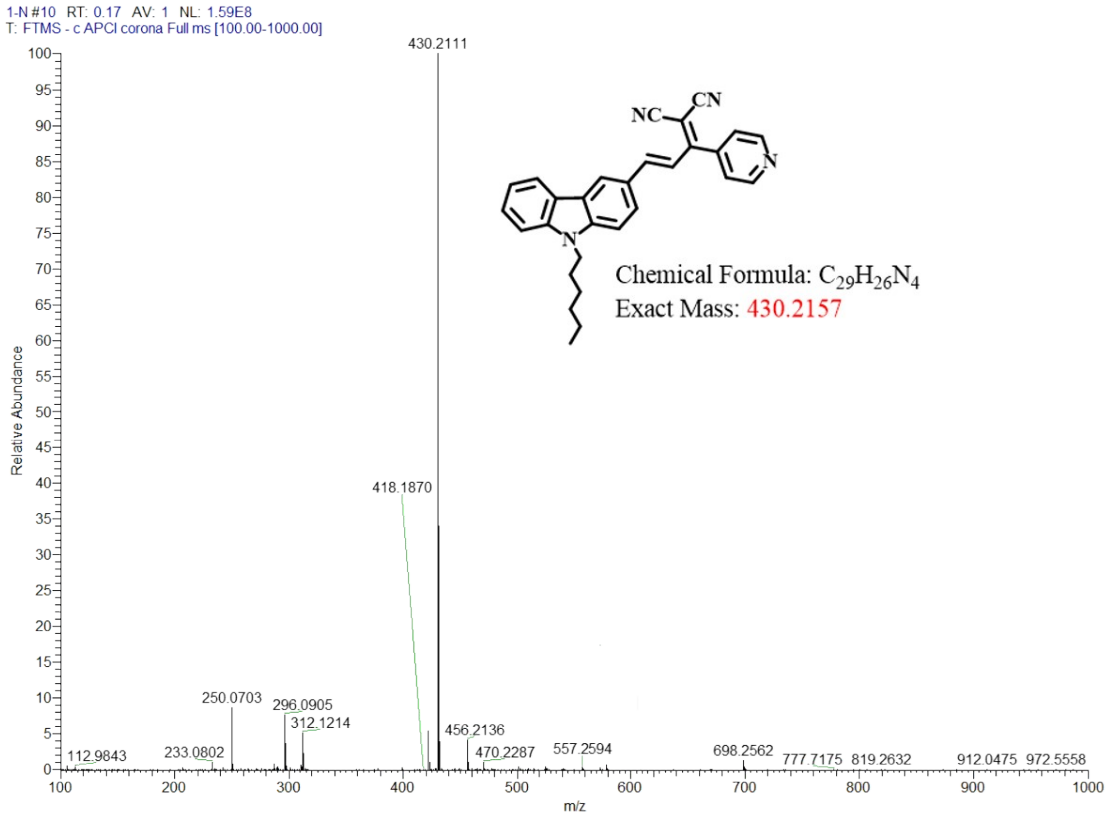

Fig S5. HRMS spectrum of **C-H**.

1.16 Synthesis of C-Br:

The synthesis step was similar to **C-H** and orange-red solid was obtained. Purified by column chromatography (petroleum ether : ethyl acetate = 15 : 1). Yield: 64%. M.p. 166-168 °C. ^{1}H NMR (400 MHz, DMSO-d_6) (**Fig S5**) δ 8.81 (d, J = 6.0 Hz, 2H), 8.62 (d, J = 1.7 Hz, 1H), 8.46-8.41 (m, 1H), 7.81 (dd, J = 8.8, 1.8 Hz, 1H), 7.65 (d, J = 8.7 Hz, 1H), 7.62-7.55 (m, 3H), 7.54-7.51 (m, 2H), 7.00 (d, J = 15.4 Hz, 1H), 4.36 (t, J = 7.1 Hz, 2H), 1.68 (d, J = 8.8 Hz, 2H), 1.17 (d, J = 4.5 Hz, 6H), 0.72 (d, J = 7.1 Hz, 3H). HRMS (ESI-MS) m/z: calcd for $C_{29}H_{25}BrN_4$ = 508.12, found 509.12 ([M+H]$^+$) (**Fig S6**).

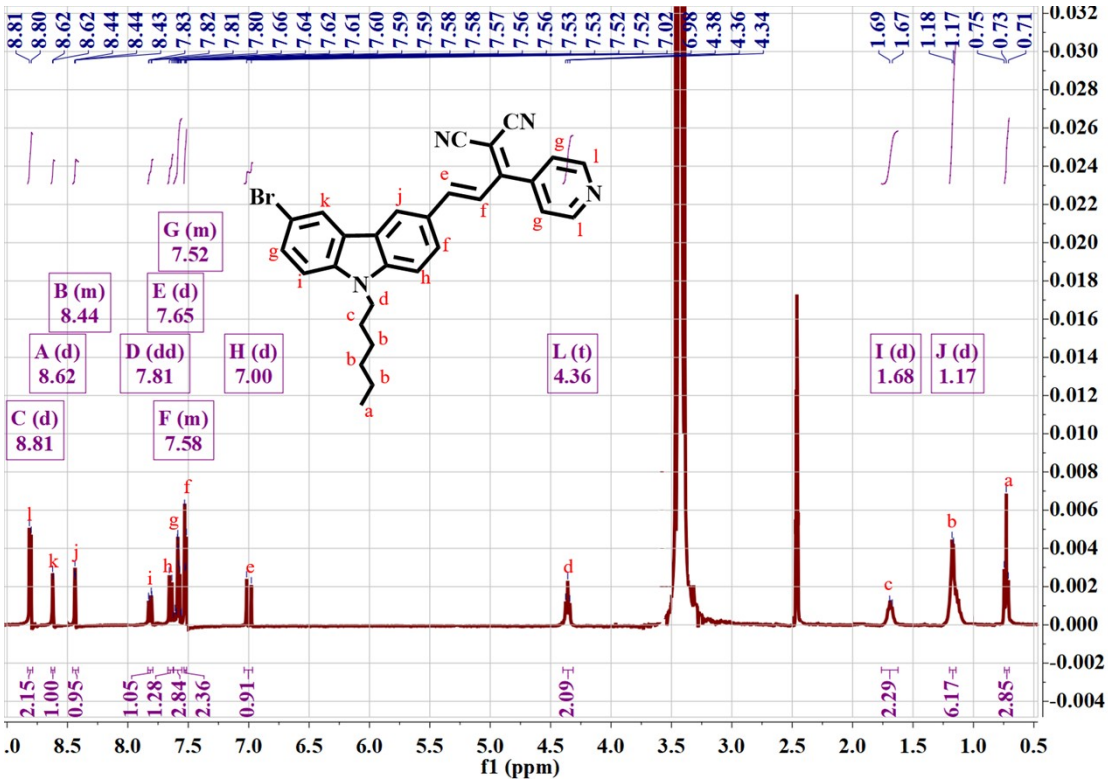

Fig S6. ^{1}H NMR spectrum of **C-Br**.

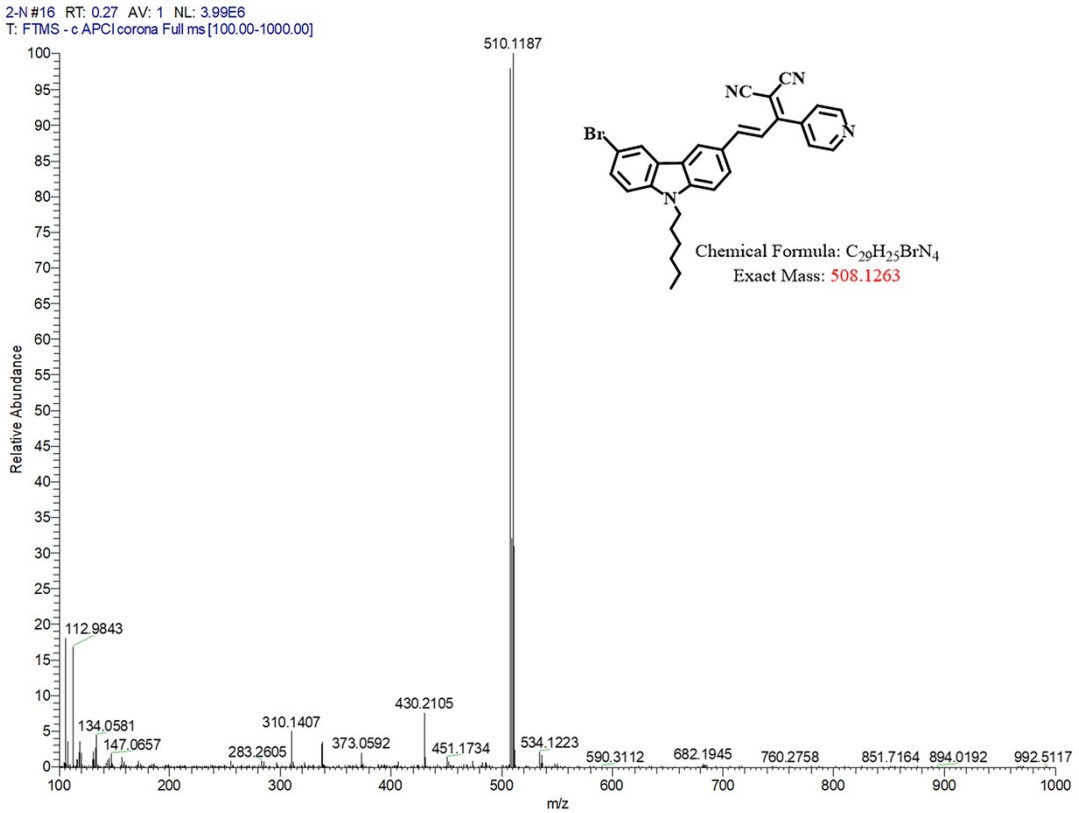

Fig S7. HRMS spectrum of **C-Br.**

1.17 Synthesis of C-I:

The synthesis step was similar to **C-H** and red solid was obtained. Purified by column chromatography (petroleum ether : ethyl acetate = 5 : 1). Yield: 52%. M.p.163-165 °C. ^{1}H NMR (400 MHz, DMSO-d_6) (**Fig S7**) δ 8.83-8.80 (m, 2H), 8.66 (d, J = 1.7 Hz, 1H), 8.61 (d, J = 1.7 Hz, 1H), 7.83 (dd, J = 8.8, 1.8 Hz, 1H), 7.76-7.70 (m, 1H), 7.65 (d, J = 8.7 Hz, 1H), 7.60-7.52 (m, 3H), 7.49 (d, J = 8.6 Hz, 1H), 7.01 (d, J = 15.4 Hz, 1H), 4.36 (t, J = 7.1 Hz, 2H), 1.73-1.64 (m, 2H), 1.25-1.14 (m, 6H), 0.78-0.72 (m, 3H). HRMS (ESI-MS) m/z: calcd for $C_{29}H_{25}IN_4$ = 556.11, found 557.11 ([M+H]$^+$) (**Fig S8**).

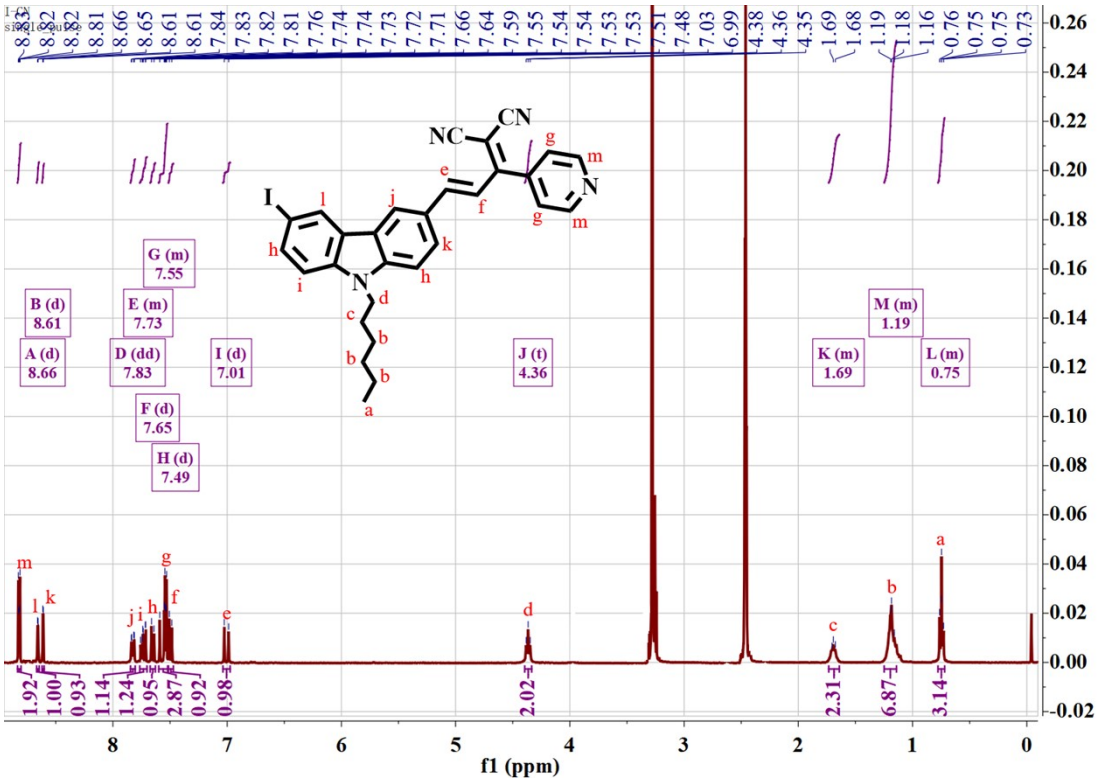

Fig S8. ^{1}H NMR spectrum of **C-I**.

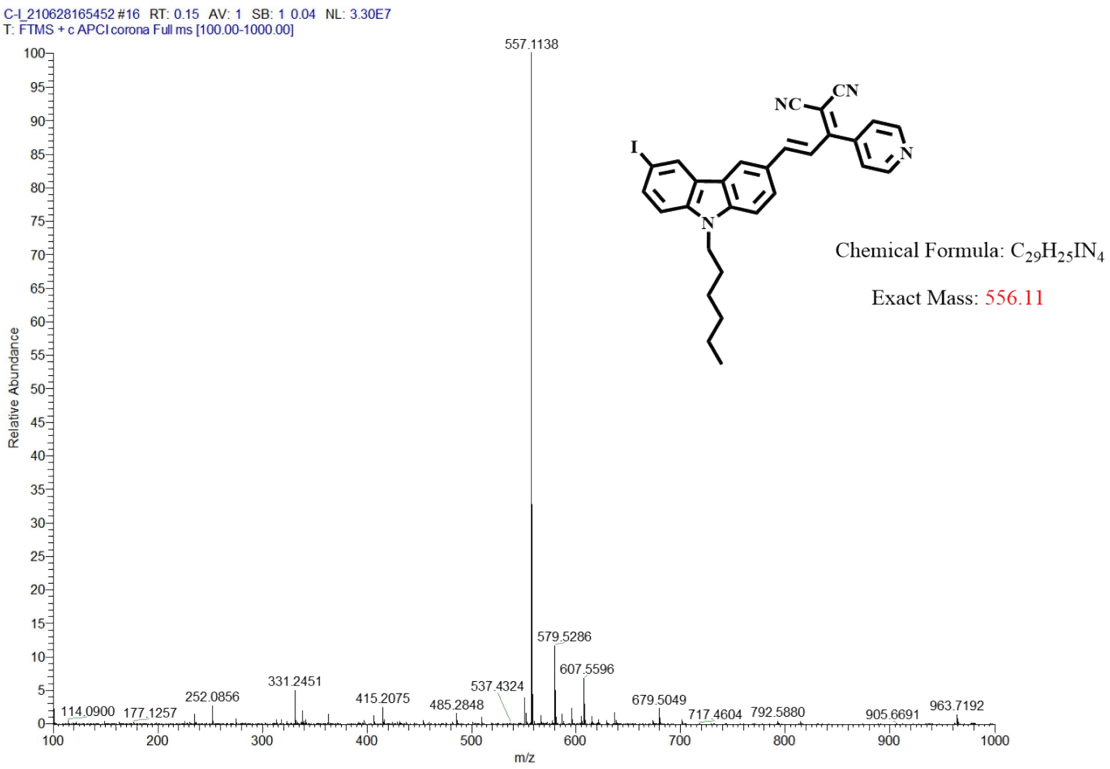

Fig S9. HRMS spectrum of **C-I.**

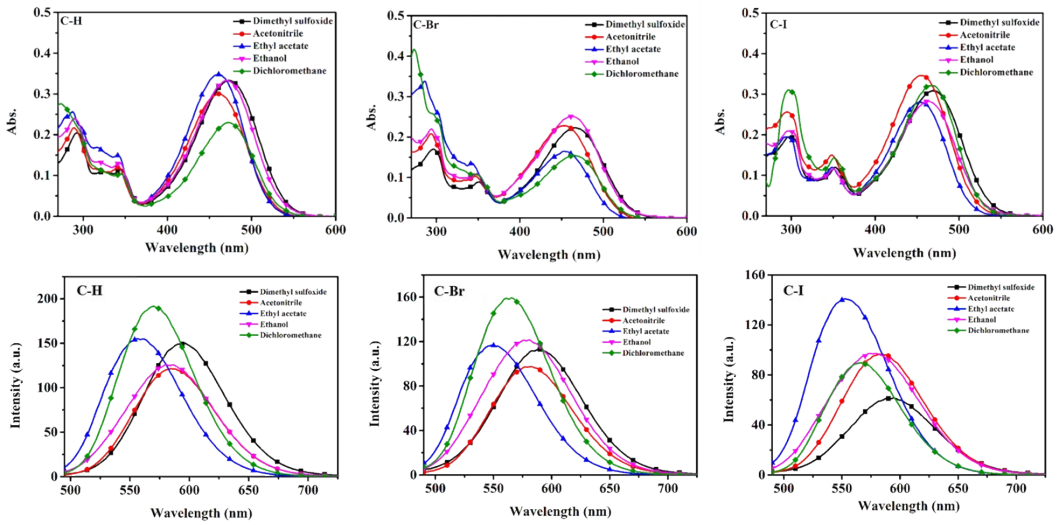

Fig S10. UV-*vis* absorption and fluorescence spectra of **C-H**, **C-Br** and **C-I** in different solvents (c = 10 μM)

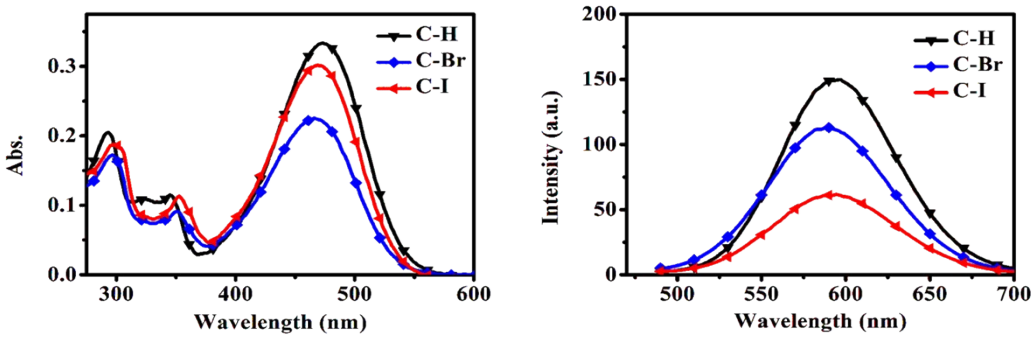

Fig S11. UV-*vis* and Single-photon fluorescence spectra of **C-H**, **C-Br** and **C-I** in DMSO solvents (c = 10 μM)

Table S1 The photophysical data of **C-H**, **C-Br** and **C-I** in different solvents. (c = 10 μM)

Cmpds	Solvents	λ_{max}^{abs}	$\varepsilon(10^4)$	λ_{max}^{em}	Φ (%)	*Stokes Shift*
C-H	Dimethyl sulfoxide	473	3.33	594	10.31	121
	Acetonitrile	461	3.01	585	8.48	124
	Ethyl acetate	461	3.48	559	10.52	98
	Ethanol	472	3.32	585	8.63	113
	Dichloromethane	472	2.23	570	10.95	98
C-Br	Dimethyl sulfoxide	467	2.22	590	6.02	123
	Acetonitrile	453	2.28	581	5.69	128
	Ethyl acetate	454	1.65	550	6.13	96
	Ethanol	462	2.53	579	6.66	117
	Dichloromethane	465	1.53	569	7.61	104
C-I	Dimethyl sulfoxide	470	3.07	594	1.68	124
	Acetonitrile	455	3.47	585	3.53	130
	Ethyl acetate	454	2.79	554	3.56	100
	Ethanol	464	2.81	578	3.96	114
	Dichloromethane	468	3.22	567	4.44	99

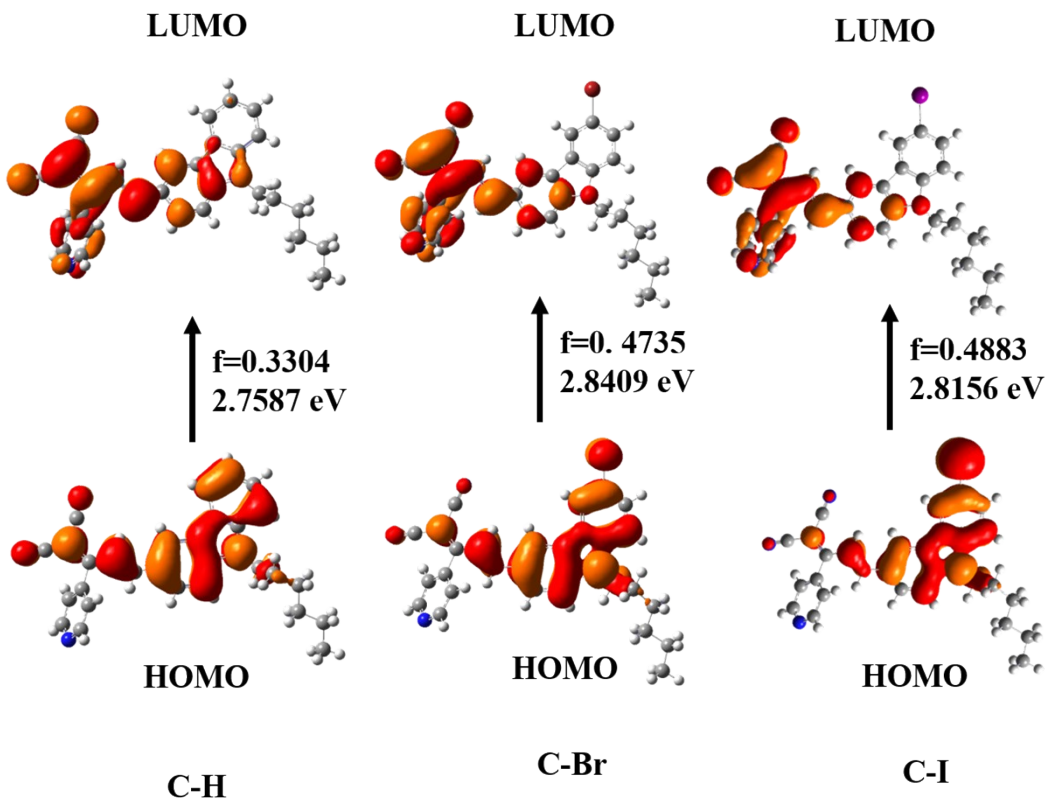

Fig S12. Molecular orbital energy diagrams for **C-H**, **C-Br** and **C-I** complex.

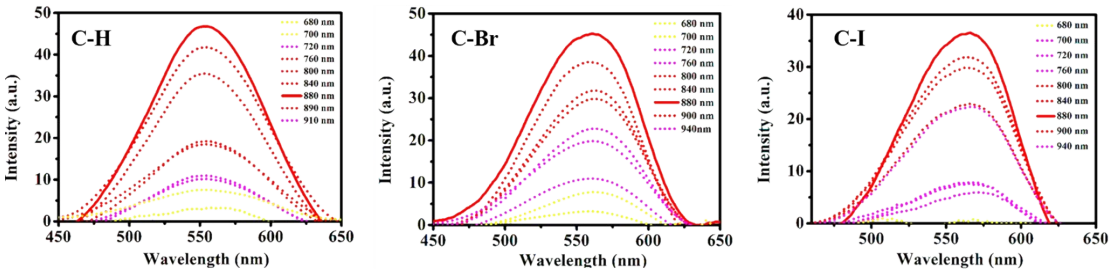

Fig S13. Two-photon emission spectra of **C-H**, **C-Br** and **C-I** in DMSO (c = 1.0 mM).

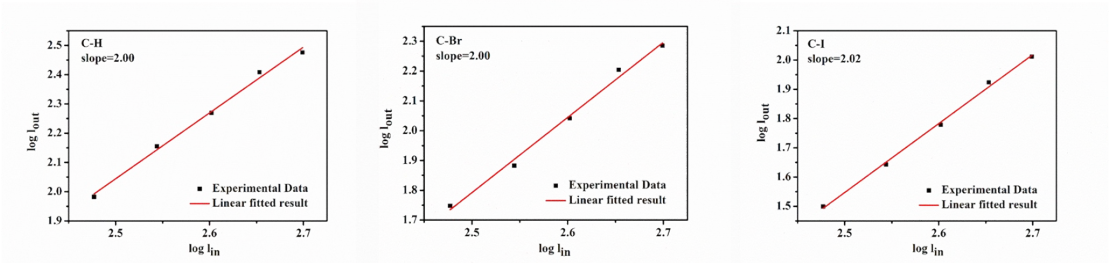

Fig S14. Two-photon absorption verification of **C-H**, **C-Br** and **C-I** which I_{in} and I_{out} represent the input laser power and output fluorescence, respectively (1 mM)

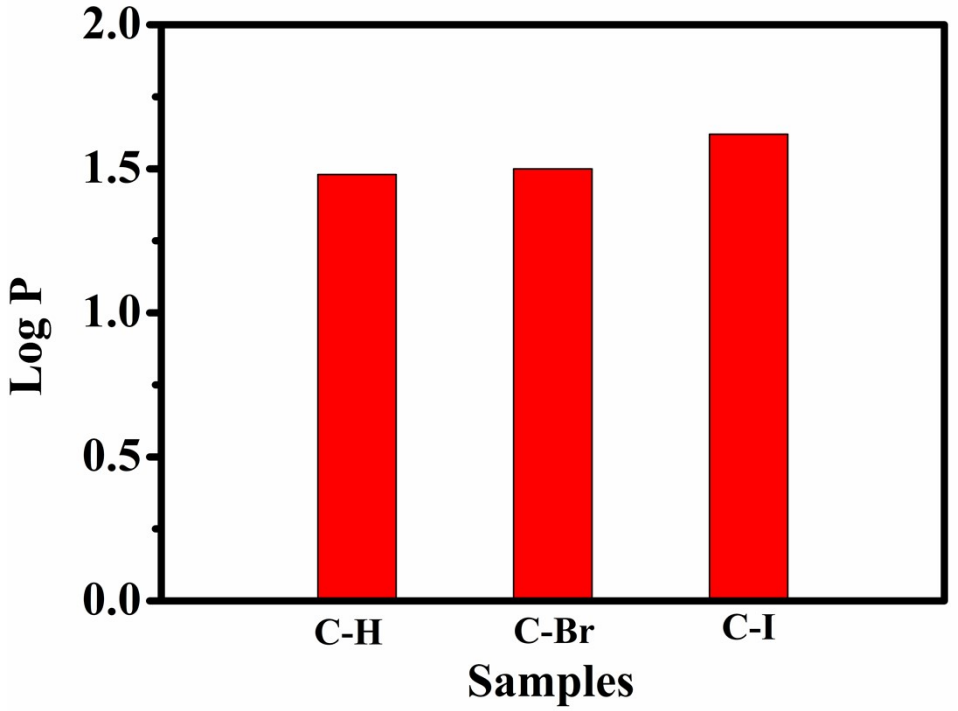

Fig S15. Octanol value of compounds.

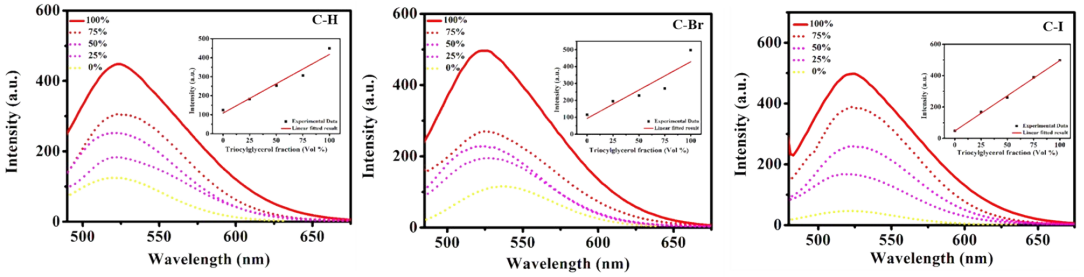

Fig S16. Emission spectra of **C-H**, **C-Br** and **C-I** in PBS with different trioctanoin ratio.

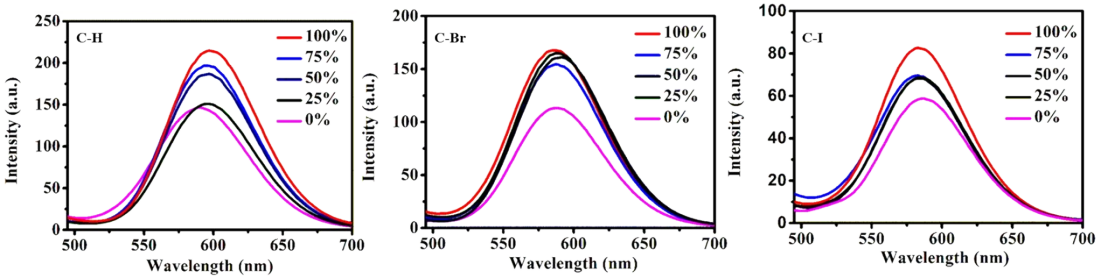

Fig S17. PL spectra of **C-H**, **C-Br** and **C-I** (10 μM) in PBS with different glycerol fractions.

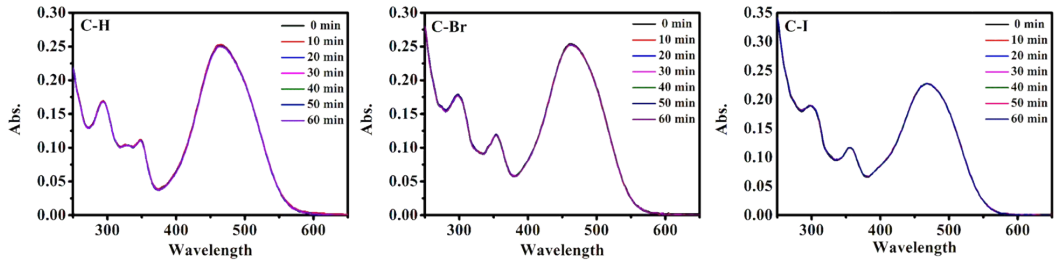

Fig S18. Time evolution of UV-vis absorption spectra of **C-H**, **C-Br** and **C-I** in PBS buffers. (c = 10 μM)

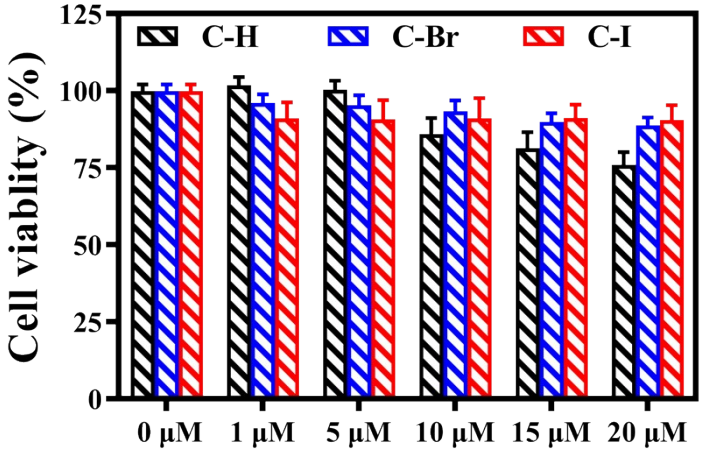

Fig S19. Cytotoxicity data of **C-H**, **C-Br** and **C-I** obtained from the MTT assay.

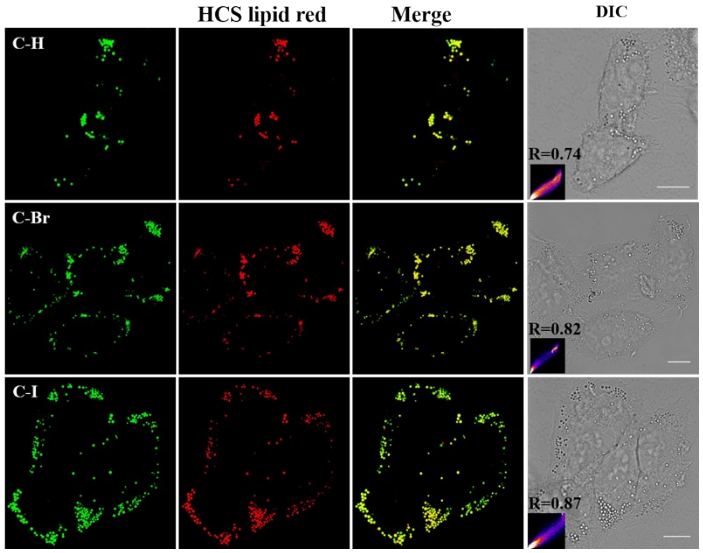

Fig S20. Determination of intercellular localization of **C-H**, **C-Br** and **C-I** by confocal microscopy in HeLa cells. Including colocalization images of HeLa cells stained with HCS deep red (0.5 μM, red channel, λ_{ex} = 633 nm, λ_{em} = 650 nm), **C-H**, **C-Br**, **C-I** (10 μM, green channel, λ_{ex} = 470 nm, λ_{em} = 580 ± 20 nm) and the merged image (yellow channel) and the bright-field image of **C-H**, **C-Br** and **C-I**, insert: pearson coefficient. Scale bar: 10 μm.

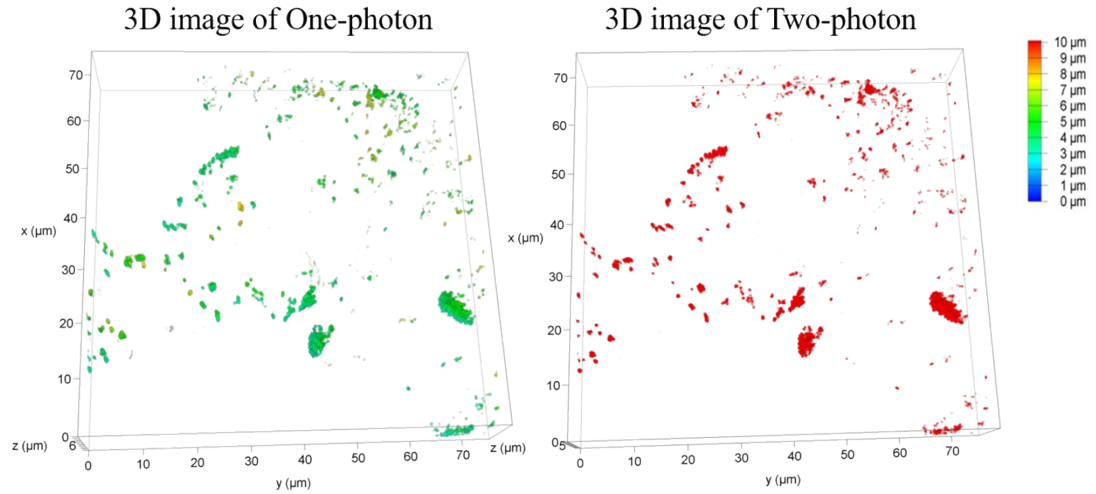

Fig S21. 3D image of One-photon (λ_{ex} = 470 nm, λ_{em} = 594nm) and two-photon fluorescence imaging (λ_{ex} = 880 nm, λ_{em} = 594 nm), scale bar: 5 μm.

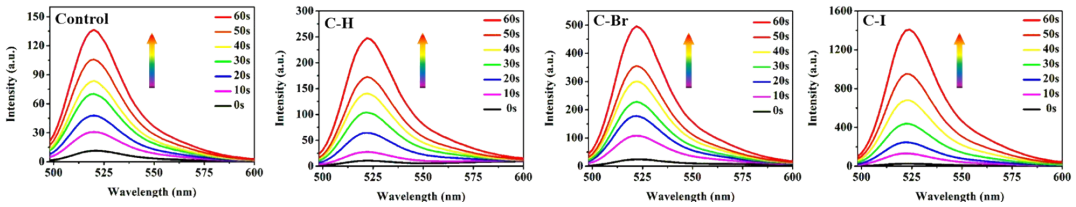

Fig S22. The change of FL intensity of complexes **C-H**, **C-Br** and **C-I** with **DCFH-DA** under diferent lighting times.

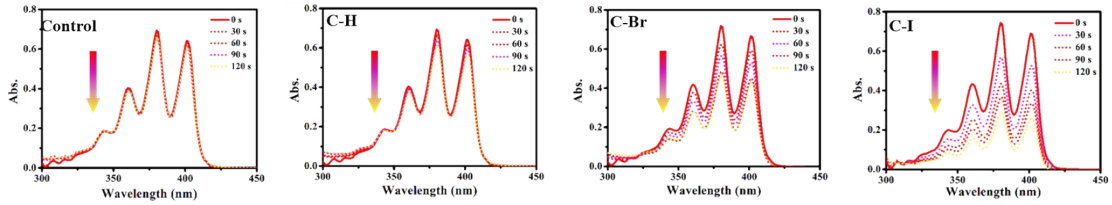

Fig S23. The UV-vis absorption spectra of complexes **C-H**, **C-Br** and **C-I** with ABDA under diferent lighting times.

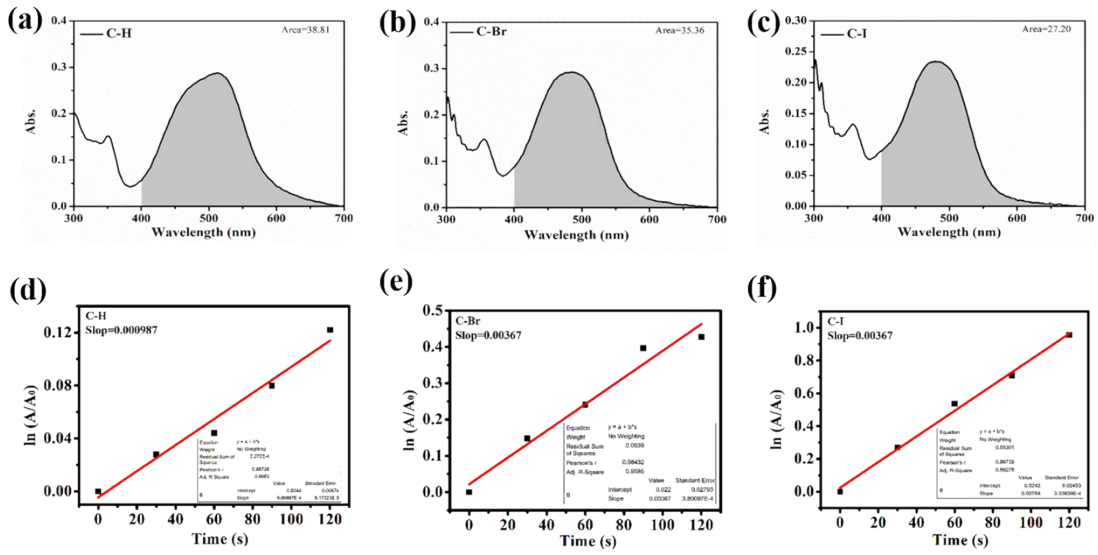

Fig S24. Chemical trapping measurements of the $^1O_2$ quantum yield. (a) The absorption peak area of **C-H**; (b) The absorption peak area of **C-Br**; (c) The absorption peak area of **C-I**; (d) The decomposition rate constants of ABDA by **C-H**; (e) The decomposition rate constants of ABDA by **C-Br**; (f) The decomposition rate constants of ABDA by **C-I.**

Table. S2 The $^1O_2$ generation ability of complexes **C-H**, **C-Br** and **C-I** in PBS buffer

	RB	**C-H**	**C-Br**	**C-I**
K	0.004	0.001	0.0036	0.0078
A/(GM)	10.94	38.81	35.36	27.20
Φ	0.75	0.052	0.21	0.59

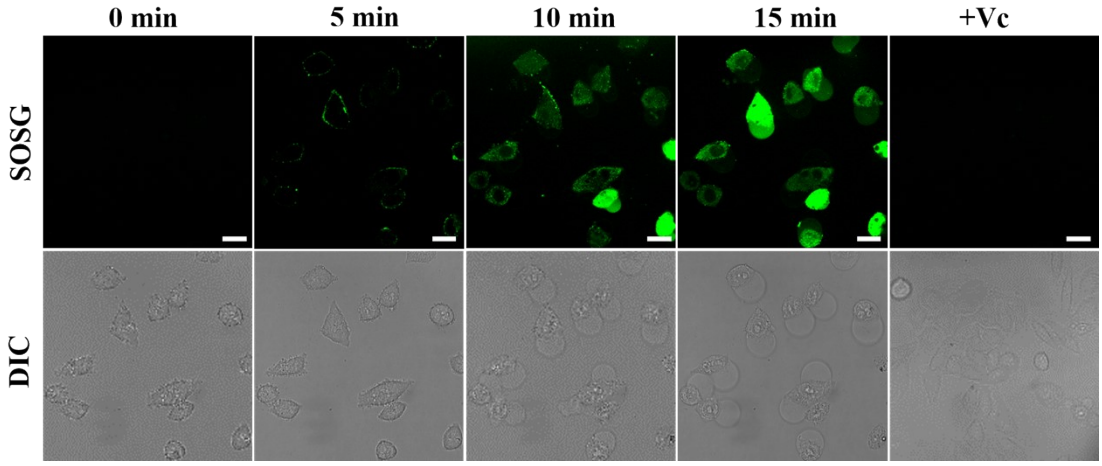

Fig S25. ROS detection in HeLa cells using SOSG as the $^1O_2$ probe (Vc was used as the specific scavenger for $^1O_2$). λ_{ex}: 880 nm, 100 mW/cm^2, scale bar: 20 μm.

Table. S3 Crystal data collection and structure refinement of **C-Br**

Comp.	**C-Br**
Empirical formula	$C_{25}H_{29}N_4Br$
CCDC	2095605
Formula weight	509.44
Temperature	296 K
Space group	P_{bcn}
Crystal system	Orthorhombic
a/Å	15.942(3)
b/Å	23.548(5)
c/Å	13.585(3)
V/Å^3	5099.8(18)
Z	8
D calcd [Mg·m^{-3}]	1.327
μ [mm^{-1}]	1.636
F（000）	2096.0
R_1	0.0685
wR_2	0.1698
Goodness-of-fit on F^2	1.207

Table S4. Selection bond lengths (Å) and angles (°) of **C-Br**

Br-C4	1.906(5)	C1-N1-C13	126.4(4)
N1-C1	1.389(6)	C12-N1-C13	125.0(5)
N1-C12	1.374(6)	N1-C1-C6	109.1(4)
N1-C13	1.452(6)	C2-C1-N1	129.4(5)
N3-C28	1.120(6)	C2-C1-C6	121.5(5)
N4-C29	1.134(7)	C3-C2-C1	117.9(5)
C1-C2	1.387(7)	C2-C3-C4	120.6(5)
C1-C6	1.414(6)	C3-C4-Br	118.5(4)
C2-C3	1.376(7)	C5-C4-Br	118.8(4)
C3-C4	1.387(7)	C5-C4-C3	122.6(5)
C4-C5	1.383(7)	C4-C5-C6	117.4(5)
C5-C6	1.388(7)	C1-C6-C7	106.4(4)
C6-C7	1.447(6)	C5-C6-C1	120.0(4)
C7-C8	1.391(6)	C5-C6-C7	133.6(4)
C7-C12	1.411(6)	C8-C7-C6	133.3(5)
C8-C9	1.395(7)	C8-C7-C12	120.4(5)
C9-C10	1.416(7)	C7-C8-C9	118.9(5)
C9-C19	1.457(6)	C8-C9-C10	119.3(4)
C10-C11	1.373(7)	C8-C9-C19	123.3(5)
C11-C12	1.394(7)	N1-C12-C7	109.7(4)
C13-C14	1.512(11)	N1-C12-C11	128.9(5)
C14-C15	1.534(9)	N1-C13-C14	118.4(6)
C15-C16	1.504(10)	C16-C15-C14	113.2(8)
C16-C17	1.479(11)	C17-C16-C15	116.2(9)
C17-C18	1.496(13)	C20-C19-C9	128.0(5)
C19-C20	1.335(7)	C27-C21-C20	122.2(5)
C20-C21	1.442(6)	C27-C21-C22	118.9(6)
C21-C22	1.518(8)	C23-C22-C21	116.7(8)
C21-C27	1.365(7)	C21-C27-C28	122.0(5)
C27-C28	1.442(7)	N3-C28-C27	177.7(7)
C27-C29	1.435(8)	N4-C29-C27	178.0(7)

[1] A. Becke, *J. Chem. Phys*., 1993, **98**, 5648-5652.

[2] Q. Zhang, X. Lu, H. Wang, H. P. Zhou, J. Y. Wu, Y. P. Tian, *Chem. Commun.*, 2018, **54**, 3771-3774.

[3] Y. Shen, T. Shao, B. Fang, W. Du, M. Z. Zhang, J. J. Liu, J. Y. Wu, Y. P. Tian, *Chem. Commun.*, 2018, **54**, 11288-11291.

[4] B. Ni, H. Z. Cao, C. K. Zhang, S. L. Li, D. D. Li, J. Y. Wu, Y. P. Tian, *Inorg. Chem*., 2020, **59**, 13671-13678.

[5] Z. Zheng, T. F. Zhang, H. X. Liu, Y. C. Chen, R. T. Kwok, C. Ma, *ACS Nano*., 2018, **12**, 8145-8159.

[6] S. L. Yi, Z. Lu, J. Zhang, J. Wang, Z. H. Xie, L. X. Hou, *ACS Appl Mater Interfaces.*, 2019, **11**, 15276-15289.